NUMERICAL SIMULATION AND RF MODEL MEASUREMENTS OF THE NEW GSI IH-DTL*

B. Krietenstein, T. Weiland, TH Darmstadt, Darmstadt, Germany
U. Ratzinger, R. Tiede, GSI, Darmstadt, Germany
S.A. Minaev, MEPhI, Moscow, Russia

Abstract

Two IH drift tube linacs (IH1 and IH2) will be part of the new high current injector of the GSI accelerator facility in Darmstadt (Germany). In order to shorten the cavity design period, numerical simulations using MAFIA, as well as rf model measurements were used to determine the dimensions of these linacs.

In this paper we present results of the simulations and the measurements for IH1, which was the more complex structure.

1 INTRODUCTION

The main parts of the GSI accelerator facility are a heavy ion linear accelerator (UNILAC), a heavy ion synchrotron (SIS) and an experimental storage ring (ESR). To be able to fill the SIS up to its space charge limit, the first (prestripper) part of the UNILAC has to be replaced (see also [2], [3]). Besides an IH RFQ and an IH superlens, two IH drift tube linacs (IH1 and IH2) will be part of the new prestripper linac. They are designed to provide an effective voltage gain of $40.8\,\mathrm{MV}$(IH1) and $42.4\,\mathrm{MV}$, respectively, at a resonance frequency of $36.136\,\mathrm{MHz}$.

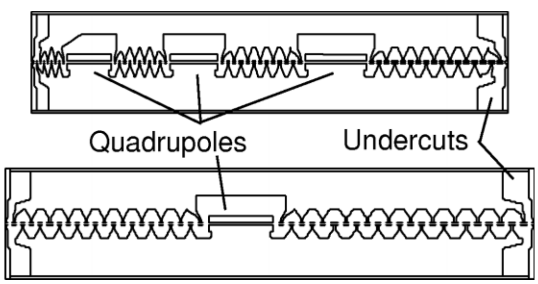

Figure 1: Layout of IH1 and IH2 after the optimization with MAFIA.

The design of these cavities based on numerical simulations using MAFIA[1] and measurements of a 1:5.88 scaled rf model. The main purpose of the simulations was the determination of main geometric parameters as the tank radius and the dimensions of the undercuts in the girders at the ends of the tanks. Furthermore, the initial guess for the capacity distribution along the drift tube structure could be improved in order to get a good start for the measurements. With help of the measurements, the gap voltage distribution could be optimized and the performance of tuning elements was studied.

The beam energy along tank IH1 ranges from $120\,\mathrm{keV/u}$ to $748\,\mathrm{keV/u}$. This range has not yet been covered by a single IH cavity of this type. Thus, the design was more difficult, especially as the gap voltage distribution given by LORASR beam dynamics calculations was not trivial.

2 SIMULATION

The procedure for the simulation was presented in [4]. As the longitudinal cut plane through the girders is a symmetry plane, only one half of the cavities had to be simulated. The main task herein is the calibration of the drift tubes for the calculation. Restrictions in memory size and computation time determine a rather coarse mesh in the drift tube region. The drift tubes consist of a tube and asymmetric bulges at the apertures for compensation of dipole components in the electric field (see also [6]). For the simulation, these tubes were replaced by tubes with octagonal cross-sections. These substitutes can be modeled with a 6×6 grid in the cross-section.

Table 1: Some data concerning the simulations.

Number of mesh points:	2-3 million
CPU-time:	36 hours
Machine:	IBM RS-6000 590

Furthermore, there are three drift tube sizes in tank IH1. Gaplengths and periodlengths at the low energy end of the tank are about 2-2.5 times smaller than at the high energy end. The correlated higher capacitive load at the entrance is partially compensated by the use of a quadrupole lens array, which allows to reduce the drift tube apertures at the low energy end. To avoid small meshsteps all drift tubes were modeled with the same radii. The change in the drift tube capacities then was compensated by variation of the gaplengths in the range of $\pm20\%$.

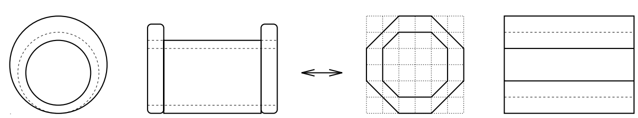

Figure 2: The real drift tube and its substitute. The octogonal cross-section can be discretized with only 3 cells along the radius.

3 SINGLE GAP INVESTIGATIONS

When designing an IH drift tube linac, it is important to know the characteristics of the gaps. Single gaps can be investigated as slices of the tank, measured from one drift tube center to the next, with magnetic boundary conditions ($\vec{B}_{\parallel} = 0$) in the cutting plane.

* work supported by GSI - Gesellschaft für Schwerionenforschung, Darmstadt, Germany

[1] Solution of **M**axwell's equations using a **F**inite **I**ntegration **A**lgorithm (see [1]).

In the following, we present results of single gap investigations for tank IH2.

3.1 Empty Tank

The fundamental mode of a cylindrical cavity is the H_{111}-Mode. With r being the cavity radius and L the cavity's length, the resonance frequency f writes

$$f = \frac{c_0}{2\pi}\sqrt{\left(\frac{\pi}{L}\right)^2 + \left(\frac{1.841}{r}\right)^2} \qquad (1)$$

In the case of single slices with magnetic boundary conditions, $L \to \infty$ and f becomes

$$f = \frac{1.841 \cdot c_0}{2\pi r} \qquad (2)$$

3.2 Tank with Girders

When girders are inserted, the capacity rises and the frequency decreases. Figure 3 shows, how the frequency varies with the girder distance

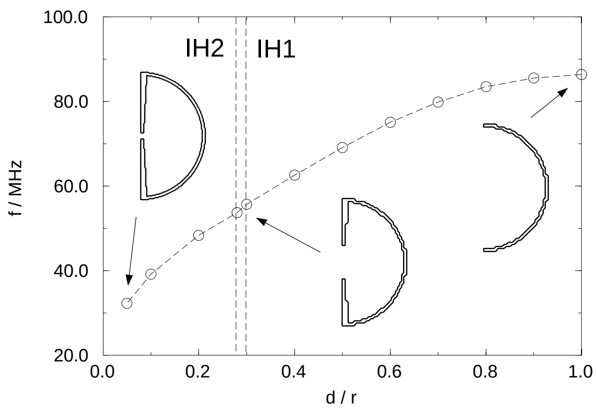

Figure 3: Variation of the resonance frequency with the distance of the girders. $d/r = 0.275$ is the distance of the girders in cavity IH2.

3.3 Tank with Drift Tubes Mounted on the Girders

The resonance frequency of a cavity slice with girders only is independent of the period length of the cell. When drift tubes are mounted with feet on the girders, the combination of period and gap length determines the frequency, which is further decreased. Figure 4 displays the frequencies of all gaps of cavity IH2.

These frequencies can be used to obtain a guess for the resonance frequency of the complete cavity IH2. If the frequencies are weighted linearly with the period lengths of the corresponding gaps:

$$f = \frac{1}{L}\sum_{i=1}^{N_{\text{Gaps}}} f_i \cdot l_i = 36.191\,\text{MHz} \qquad (3)$$

L denotes the cavity length, f_i and l_i the frequency and period length of the indexed gap, respectively. The value for the frequency only differs from the actually measured

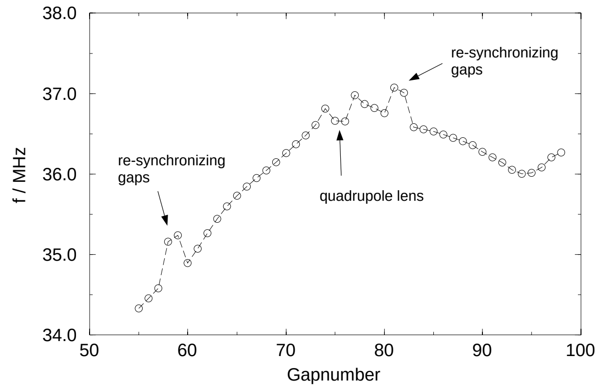

Figure 4: Local frequencies of all gaps of cavity IH2. The values result from single gap calculations.

and simulated frequency by less then half a percent, but this method does not include the effect of undercuts in the girders, which also decrease the frequency of the cavity.

For a direct comparison, table 2 shows, how the frequency changes in cavity IH2, when girders, drift tubes and their feet are mounted.

Table 2: Decrease in frequency, when girders, drift tubes and their feet are mounted.

Step	Frequency / MHz	Deviation
Empty cavity	86.373	0%
Girders added	53.698	-37.8%
Drift tubes and feet added	36.191 (34.332-36.979)	-58.1% (-60.3%-57.2%)

4 MEASUREMENTS

For the measurements at GSI, the perturbation method was used. The perturbing bead was a silver sphere of $2.5\,\text{mm}$ radius for the measurements of tank IH2. As the drift tube apertures were too small in tank IH1, a metal cylinder of the same length, but only $0.8\,\text{mm}$ diameter was used in order to get reliable results. Goals for the measurement were

- Determination of the resonance frequency
- Measuring and optimizing the gap voltage distribution
- Obtaining frequency range and gap voltage distortion of the tuning elements

The gap voltage distribution could be optimized within 5 steps by variation of the drift tube lengths, keeping the period lengths constant. The asymmetric gap geometry at the end of each drift tube containing a quadrupole triplet lens caused asymmetric electric gap fields with peaks close to the slim drift tube. A conical drift tube shape was introduced for these gaps, which makes the electric field distribution along the beam axis more symmetric (see figure 5).

The tuning method for tank IH1 will be the same as for tank IH2 (see [4]). Three plungers have successfully been tested. They are positioned between the quadrupole lenses and in the high energy section of IH1. A plunger at the low energy end showed a rupture in the tuning characteristics.

This was caused by a plunger resonance, which split the operating mode in a higher and a lower mode. For this reason, no plunger will be used at that position. The gap field distortion at the nominal frequency is neglectable.

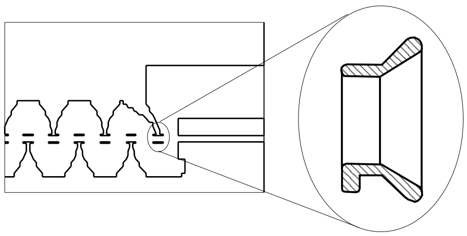

Figure 5: Conical drift tubes are used near the quadrupole lenses in order to reduce the peak field.

5 RESULTS

Figure 7 compares the simulated, the measured and the reference gap voltage distribution. In the fifth and final optimization step, the deviation of the measured voltages was $< 1\%$. The simulation's deviation is up to 15%. This is plausible, as the distribution reacts very sensitive on changes in the drift tube geometry and can be modified, even after the cavity is assembled. Figure 6 compares the deviation of the measured and the reference voltage for two optimization steps and the change in gaplengths between these two steps. Figure 6 demonstrates, how the gap voltage distribution can be tilted by variation of the drift tube geometries.

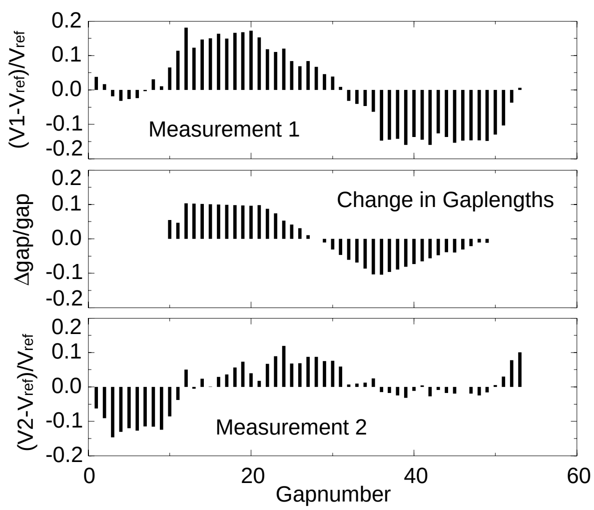

Figure 6: Relative deviation of the measured and the reference voltage distribution for two measurements and the relative change in the gaplengths between these measurements.

The more important point was the accuracy of the resonance frequency, as tuning was planned in the range from 0% to -0.5% only. Table 3 lists measured and calculated frequencies of the operating modes of tanks IH1 and IH2, respectively. Due to the detailed calibration of the drift tube substitutes, the agreement is excellent.

6 SUMMARY

With the help of measurements and simulations, the design of two new IH drift tube linacs could be completed within

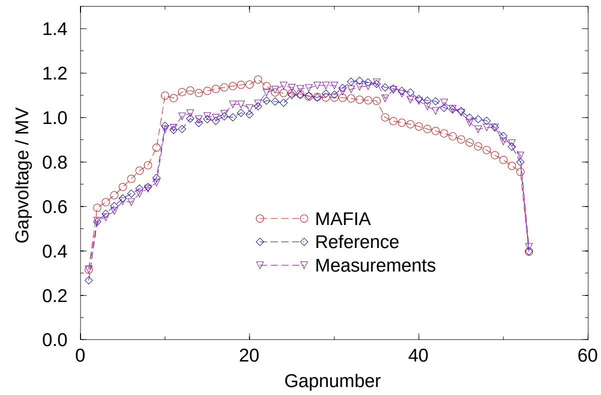

Figure 7: Calculated, measured and reference gap voltage distribution in cavity IH1

Table 3: Calculated and measured frequencies of the operating modes of IH1 and IH2

	IH1	IH2
MAFIA	36.255	36.275
Measurement	36.195	36.287
Rel. Dev. [%]	0.16%	0.03%

the project's schedule. The tanks and the girder structure could be ordered, even before the measurements started. While measured and simulated voltage distributions differ slightly, the frequencies agree very well.

It could be shown, that even such complex structures as tank IH1 with its three quadrupole lenses can be simulated numerically with good results.

7 REFERENCES

[1] The MAFIA collaboration, *User's Guide MAFIA Version 3.2*, CST GmbH, Lauteschlägerstraße 38, D-64289 Darmstadt, Germany.

[2] *Beam Intensity Upgrade of the GSI Accelerator Facility*, GSI-95-05, Report, June 1995, ISSN 0171-4546

[3] U. Ratzinger, *The New Prestripper Linac for High Current Heavy Ion Beams*, Proceedings of the XVIII International Linear Accelerator Conference, August 1996, Geneva, Switzerland, vol. 1, p. 288-292.

[4] B. Krietenstein, S.A. Minaev, U. Ratzinger, R. Tiede, T. Weiland, *Numerical Simulation of IH-accelerators with MAFIA and RF Model Measurements*, Proceedings of the XVIII International Linear Accelerator Conference, August 1996, Geneva, Switzerland, vol. 1, p. 243-245.

[5] E. Nolte et alt., *The Munich Heavy Ion Postaccelerator*, Nuclear Instruments and Methods 158 (1979),pp. 311-324

[6] U. Ratzinger, *Interdigital RF Structures*, Proceedings of the Linear Accelerator Conference 1990, Albuquerque, New Mexico, LA-12004-C, pp. 525-529.